

# Universal Steps in Quantum Dynamics with Time-Dependent Potential-Energy Surfaces: Beyond the Born-Oppenheimer Picture

Guillermo Albareda,<sup>1,\*</sup> Ali Abedi,<sup>2,†</sup> Ivano Tavernelli,<sup>3,‡</sup> and Angel Rubio<sup>2,4,§</sup>

<sup>1</sup>*Departament de Química Física & Institut de Química Teòrica i Computacional, Universitat de Barcelona, 08028 Barcelona, Spain*

<sup>2</sup>*Nano-Bio Spectroscopy Group and ETSF, Dpto. Física de Materiales, Universidad del País Vasco, CFM CSIC-UPV/EHU-MPC & DIPC, 20018 San Sebastián, Spain.*

<sup>3</sup>*IBM Research GmbH, Zürich Research Laboratory, 8803 Rüschlikon, Switzerland*

<sup>4</sup>*Max Planck Institute for the Structure and Dynamics of Matter and Center for Free-Electron Laser Science, Luruper Chaussee 149, 22761 Hamburg, Germany.*

In the conditional approach to molecular dynamics the electron-nuclear wavefunction is exactly decomposed into an ensemble of nuclear wavepackets governed by conditional time-dependent potential-energy surfaces (C-TDPESs) [G. Albareda, et al., Phys. Rev. Lett. 105, 123002 (2014)]. Employing a one-dimensional model system we show that for strong nonadiabatic couplings the C-TDPESs exhibit steps that bridge between piecewise adiabatic shapes. By a detailed analysis of the steps, we discuss the ultimate nature of electron-nuclear correlations and by comparing them with the discontinuities of the exact time-dependent potential-energy surface of the exact factorization approach we elaborate on the universality of this feature when a single time-dependent potential-energy surface governs the nonadiabatic nuclear dynamics.

PACS numbers: 31.15.-p, 31.15.X-, 31.50.-x, 31.15.A-

The description of correlated electron-nuclear dynamics remains a formidable challenge in condensed-matter physics and theoretical chemistry [1–6]. Relying on the Born-Huang expansion of the full molecular wavefunction, a majority of approaches that provide a numerically accurate description of the so-called “nonadiabatic” processes require the propagation of a set of many-body nuclear wavepackets on a coupled set of Born-Oppenheimer potential-energy surfaces (BOPEs) [7–13]. Whenever electron-nuclear coherence effects are unimportant, efficient mixed quantum-classical propagation techniques can be used [14–20]. However, in order to account for strong correlations, the access to quantum features of the nuclear motion such as spreading, tunnelling or splitting is crucial. Hence, a reliable description of molecular dynamics becomes very expensive due to the calculation of the full BOPEs, a (time-independent) problem that scales exponentially with both the nuclear and electronic degrees of freedom [21–23]. Towards a more efficient description of correlated electron-nuclear dynamics, avoiding the computational costs of calculating the BOPEs and non-adiabatic couplings, two alternative formally exact frameworks, viz. the exact factorization (EF) [24] and the conditional decomposition (CD) [25], have been recently proposed.

The CD approach to molecular dynamics allows for the decomposition of the electron-nuclear wavefunction into an ensemble of nuclear wavefunctions effectively governed by conditional time-dependent potential-energy surfaces (C-TDPESs) [25]. While keeping the theory at the full configuration level, this approach allows for the use of trajectory-based statistical techniques to circumvent the

calculation of the BOPEs and nonadiabatic couplings. Furthermore, this approach avoids artifacts coming from the tracing out of the electronic degrees of freedom and, hence, it allows to draw clear connections between different formally exact frameworks. In this Letter we investigate the generic features of the exact C-TDPESs in the presence of strong nonadiabatic couplings. A major result will be that the exact C-TDPESs exhibit discontinuous steps connecting different BOPEs analogous to paradigmatic feature of the effective time-dependent potential that governs the nuclear dynamics in the EF framework. By establishing a formal connection between the CD and the EF frameworks we will elaborate on the universality of this feature.

Throughout this Letter we use atomic units, and electronic and nuclear coordinates are collectively denoted by  $\mathbf{r} = \{\mathbf{r}_1, \dots, \mathbf{r}_{N_e}\}$  and  $\mathbf{R} = \{\mathbf{R}_1, \dots, \mathbf{R}_{N_n}\}$ , where  $N_e$  and  $N_n$  are the total number of electrons and nuclei. We have recently proved [25] that the full (non-relativistic) electron-nuclear wavefunction  $\Psi(\mathbf{r}, \mathbf{R}, t)$  can be exactly decomposed into an ensemble of conditional nuclear wavefunctions,  $\psi_\alpha(\mathbf{R}, t) := \int \delta(\mathbf{r}_\alpha(t) - \mathbf{r}) \Psi(\mathbf{r}, \mathbf{R}, t) d\mathbf{r}$ , provided that the electronic trajectories  $\{\mathbf{r}_\alpha(t) \equiv \mathbf{r}_{1,\alpha}(t), \dots, \mathbf{r}_{N_e,\alpha}(t)\}$  explore the electronic support of  $|\Psi(\mathbf{r}, \mathbf{R}, t)|^2$  at any time  $t$  [26]. These conditional wavefunctions can be used to reconstruct the full wavefunction (or equivalently any observable) through  $\Psi(\mathbf{r}, \mathbf{R}, t) = \hat{\mathcal{D}}_{\mathbf{r}}[\psi_\alpha]$ , where  $\hat{\mathcal{D}}_{\mathbf{a}}[f(\mathbf{a}_\alpha)] \equiv \sum_{\alpha=1}^{\infty} \delta(\mathbf{a}_\alpha - \mathbf{a}) f(\mathbf{a}_\alpha) / \sum_{\alpha=1}^{\infty} \delta(\mathbf{a}_\alpha - \mathbf{a})$  when  $\sum_{\alpha=1}^{\infty} \delta(\mathbf{a}_\alpha - \mathbf{a}) \neq 0$  and it is zero otherwise. Throughout this work we will use quantum trajectories defined through  $\mathbf{r}_{\xi,\alpha}(t) = \mathbf{r}_{\xi,\alpha}(t_0) + \int_{t_0}^t \dot{\mathbf{r}}_{\xi,\alpha}(t') dt'$

and  $\mathbf{R}_{\nu,\alpha}(t) = \mathbf{R}_{\nu,\alpha}(t_0) + \int_{t_0}^t \dot{\mathbf{R}}_{\nu,\alpha}(t') dt'$ , where electronic and nuclear velocities are respectively given by  $\dot{\mathbf{r}}_{\xi,\alpha} = \nabla_{\xi} S|_{\mathbf{r}_{\alpha}, \mathbf{R}_{\alpha}}$  and  $\dot{\mathbf{R}}_{\nu,\alpha} = (\nabla_{\nu} S)/M_{\nu}|_{\mathbf{r}_{\alpha}, \mathbf{R}_{\alpha}}$ , and  $S$  is the phase of the full electron-nuclear wavefunction  $\Psi = |\Psi|e^{iS}$  [27, 28]. For the sake of simplicity, we will omit from now on the explicit dependence of the trajectories on time, i.e.  $\{\mathbf{r}_{\alpha}\} \equiv \{\mathbf{r}_{\alpha}(t)\}$ . In the absence of time-dependent external fields, the system is described by the Hamiltonian  $\hat{H} = \hat{T}_e(\mathbf{r}) + \hat{T}_n(\mathbf{R}) + W(\mathbf{r}, \mathbf{R}, t)$ , where  $\hat{T}_e = -\sum_{\xi=1}^{N_e} \nabla_{\xi}^2/2$  and  $\hat{T}_n = -\sum_{\nu=1}^{N_n} \nabla_{\nu}^2/2M_{\nu}$  are the electronic and nuclear kinetic energy operators, and  $W(\mathbf{r}, \mathbf{R}, t) = W_{ee}(\mathbf{r}) + W_{nn}(\mathbf{R}) + W_{en}(\mathbf{r}, \mathbf{R})$  denotes the Coulombic interactions. The wavefunctions  $\psi_{\alpha}(\mathbf{R}, t)$  obey the equations of motion [25]:

$$id_t \psi_{\alpha}(\mathbf{R}, t) = \left\{ \hat{T}_n(\mathbf{R}) + V_{\alpha}(\mathbf{R}, t) \right\} \psi_{\alpha}(\mathbf{R}, t), \quad (1)$$

where the effective potentials  $V_{\alpha}(\mathbf{R}, t) = W_{\alpha}(\mathbf{R}, t) + K_{\alpha}(\mathbf{R}, t) + A_{\alpha}(\mathbf{R}, t)$  are named conditional time-dependent potential-energy surfaces (C-TDPESs). Each C-TDPES consists of three terms: the conditional Coulombic potential  $W_{\alpha}(\mathbf{R}, t) = W(\mathbf{r}_{\alpha}, \mathbf{R}, t)$ , the kinetic correlation potential,  $K_{\alpha}(\mathbf{R}, t) = \frac{\hat{T}_e \Psi}{\Psi}|_{\mathbf{r}_{\alpha}}$ , and an advective potential,  $A_{\alpha}(\mathbf{R}, t) = i \sum_{\xi=1}^{N_e} \frac{\nabla_{\xi} \Psi}{\Psi}|_{\mathbf{r}_{\alpha}} \cdot \dot{\mathbf{r}}_{\xi,\alpha}$ . As shown in Eq. (1), each nuclear wavefunction  $\psi_{\alpha}(\mathbf{R}, t)$  represents a  $3N_n$ -dimensional *slice* of the full molecular wavefunction (taken along the nuclear coordinates) whose evolution is, in general, non-unitary due to the complex nature of the kinetic and advective potentials.

Note that the propagation of the nuclear equations of motion in Eq. (1) does not require the calculation of the BOPEs. This makes the method particularly advantageous when studying processes that involve many BOPEs. Since the initial conditions of a trajectory-based simulation can be generated with importance-sampling techniques, conditional decompositions can be exploited to circumvent the problem of storing and propagating a many-particle wavefunction whose size scales exponentially with the number of particles. In this respect, note that the decomposition of the molecular wavefunction in Eq. (1) is only one case among many other possible conditional decompositions [25, 29–32].

To analyze the C-TDPESs, we decompose  $V_{\alpha}$  into real and imaginary parts, i.e.,  $V_{\alpha}^{\Re} = W_{\alpha}(R, t) + K_{\alpha}^{\Re} + A_{\alpha}^{\Re}$  and  $V_{\alpha}^{\Im} = K_{\alpha}^{\Im} + A_{\alpha}^{\Im}$ , where

$$K_{\alpha}^{\Re} = \sum_{\xi=1}^{N_e} Q_{\xi,\alpha}^e + \frac{(\nabla_{\xi} S)^2}{2} \Big|_{\mathbf{r}_{\alpha}}; \quad K_{\alpha}^{\Im} = - \sum_{\xi=1}^{N_e} \frac{\nabla_{\xi} \mathbf{j}_{\xi}}{2|\Psi|^2} \Big|_{\mathbf{r}_{\alpha}}, \quad (2)$$

and

$$A_{\alpha}^{\Re} = - \sum_{\xi=1}^{N_e} \nabla_{\xi} S|_{\mathbf{r}_{\alpha}} \cdot \dot{\mathbf{r}}_{\xi,\alpha}; \quad A_{\alpha}^{\Im} = \sum_{\xi=1}^{N_e} \frac{\nabla_{\xi} |\Psi|^2}{2|\Psi|^2} \Big|_{\mathbf{r}_{\alpha}} \cdot \dot{\mathbf{r}}_{\xi,\alpha}, \quad (3)$$

are respectively the real and imaginary parts of the kinetic and advective correlation potentials. In Eq. (2)

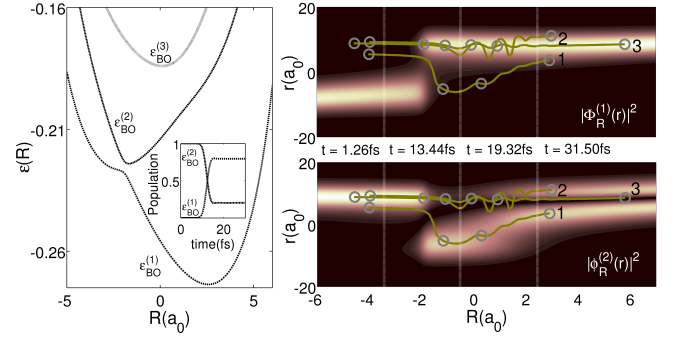


FIG. 1. Left Panel: lowest three BOPEs  $\epsilon_{BO}^{(1)}$ ,  $\epsilon_{BO}^{(2)}$ , and  $\epsilon_{BO}^{(3)}$ . In the inset: adiabatic populations as a function of time. Right Panel: Squared value of the Born-Oppenheimer states  $\Phi_R^{(1)}(r)$  and  $\Phi_R^{(2)}(r)$  along with the evolution of three selected trajectories  $\{r_{\alpha}(t), R_{\alpha}(t)\}$  labeled  $\alpha = 1, 2, 3$ . The position of these trajectories at four different times is also shown (in gray circles) for later reference.

we have respectively defined the  $\xi$ -th components of the so-called electronic quantum potential [27, 28] and the current probability density as  $Q_{\xi,\alpha}^e = -\nabla_{\xi}^2 |\Psi|/2|\Psi|_{\mathbf{r}_{\alpha}}$  and  $\mathbf{j}_{\xi} = |\Psi|^2 \nabla_{\xi} S$ . While the classical kinetic potential,  $(\nabla_{\xi} S)^2/2$ , is in general a smooth function of the nuclear coordinates, we expect the contributions,  $Q_{\xi,\alpha}^e$  and  $K_{\alpha}^{\Im}$ , to be rather “discontinuous” because of their dependence on the inverse of the nuclear probability density. Notice that these last two quantities are implicit functions of the electronic coordinates. Specifically, the electronic quantum potential  $Q_{\xi,\alpha}^e$  accounts for changes of the curvature of the full probability density along the electronic coordinates (as a function of the nuclear positions). Alternatively,  $K_{\alpha}^{\Im}$  describes the dispersion (e.g. spreading or splitting) of the full wavefunction in the electronic direction. Both contributions become large in the vicinity of a node, and thus, they will be important whenever the full probability density splits apart along the electronic coordinates. The advective correlations in Eq. (3) are weighted by the electronic velocities,  $\dot{\mathbf{r}}_{\xi,\alpha}$ , and hence, they will be significant only during a fast reconfiguration of the electronic degrees of freedom.

To study the features of the exact C-TDPESs during nonadiabatic processes in the CD approach, we employ the model introduced by Shin and Metiu [33], which consists of three ions and a single electron. Two ions are fixed at a distance  $L = 19.0a_0$ , and the third ion and the electron are free to move in one dimension along the line joining the fixed ions. The Hamiltonian for this system reads:

$$\hat{H}(r, R) = -\frac{1}{2} \frac{\partial^2}{\partial r^2} - \frac{1}{2M} \frac{\partial^2}{\partial R^2} + \frac{1}{|\frac{L}{2} - R|} + \frac{1}{|\frac{L}{2} + R|} - \frac{\text{erf}\left(\frac{|R-r|}{R_f}\right)}{|R-r|} - \frac{\text{erf}\left(\frac{|r-\frac{L}{2}|}{R_r}\right)}{|r-\frac{L}{2}|} - \frac{\text{erf}\left(\frac{|r+\frac{L}{2}|}{R_l}\right)}{|r+\frac{L}{2}|}, \quad (4)$$

where the symbols  $\mathbf{r}$  and  $\mathbf{R}$  are replaced by  $r$  and  $R$ , and the coordinates of the electron and the movable nucleus are measured from the center of the two fixed ions. We choose the remaining parameters to be the same as in reference [34], i.e.  $M = 1836a_0$  and  $R_f = 5.0a_0$ ,  $R_l = 4.0a_0$ , and  $R_r = 3.1a_0$  such that the first BOPEs,  $\epsilon_{BO}^{(1)}$ , is strongly coupled to the second,  $\epsilon_{BO}^{(2)}$  around  $R_{ac} = -2a_0$ . The coupling to the rest of the BOPEs is negligible. The time-independent electronic problem is fully characterized through the so-called electronic Hamiltonian, i.e.  $(\hat{T}_e + W)\Phi_R^{(j)}(r) = \epsilon_{BO}^{(j)}(R)\Phi_R^{(j)}(r)$ . We suppose the system to be initially excited to  $\epsilon_{BO}^{(2)}$  and the initial nuclear wavefunction to be a Gaussian wavepacket with  $\sigma = 1/\sqrt{2.85}$ , centered at  $R = -4.0a_0$ , i.e. the initial full wavefunction is  $\Psi(r, R, t_0) = A e^{-(R+4)^2/\sigma^2} \Phi_R^{(2)}(r)$  with  $A$  being a normalization constant. On the left panel of Fig. 1 we show the first three BOPEs together with the evolution of the adiabatic populations (in the inset). The right panel of Fig. 1 shows the first two Born-Oppenheimer states  $\Phi_R^{(1)}(r)$  and  $\Phi_R^{(2)}(r)$  along with the evolution of three selected trajectories  $\{r_\alpha, R_\alpha\}$  labeled  $\alpha = 1, 2, 3$  that will be used to analyse the  $\mathbb{C}$ -TDPEs. In Fig. 2 we present four time snapshots containing relevant information about the  $\mathbb{C}$ -TDPEs as well as the conditional nuclear wavefunctions. For the sake of clarity we also define approximated real and imaginary components of  $\mathbb{C}$ -TDPEs respectively as  $V_{\alpha,app}^{\Re} = Q_\alpha^e + W_\alpha$  and  $V_{\alpha,app}^{\Im} = K_\alpha^{\Im}$ .

At the initial time ( $t_0 = 0$ fs), due to the choice of  $\Psi(r, R, t_0)$ , the  $\mathbb{C}$ -TDPEs are real,  $\alpha$ -independent, and by construction all equal to the first excited BOPE  $\epsilon_{BO}^{(2)}$ :

$$V_\alpha = \frac{\hat{T}_e \Phi_R^{(2)}(r)}{\Phi_R^{(2)}(r)} \Big|_{r_\alpha} + W_\alpha = V_{\alpha,app}^{\Re} = \epsilon_{BO}^{(2)}, \quad \forall \alpha \quad (5)$$

where we used that  $Q_\alpha^e(R, t_0) = \hat{T}_e \Phi_R^{(2)}(r)/\Phi_R^{(2)}(r)$  when  $\partial_r S = 0$  (see Ref. [35]). Since  $\Psi(r, R, t_0)$  is not an eigenstate of the Hamiltonian in (4), it evolves in time. As it is made clear in the right panels of Fig. 1, at  $t = 13.44$ fs, the trajectories  $(r_2, R_2)$  and  $(r_3, R_3)$ , associated respectively with the conditional wavefunctions  $\psi_2$  and  $\psi_3$ , are running straight (i.e.  $\dot{r}_{2,3} \approx 0$ ) from the support of  $\Phi_R^{(2)}(r)$  to fall in the support of  $\Phi_R^{(1)}(r)$ . For  $\alpha = 2, 3$  the  $\mathbb{C}$ -TDPEs are real ( $V_{2,3}^{\Im} = 0$ ) and satisfy  $V_{2,3} \approx V_{2,3,app}^{\Re}$ , with  $Q_{2,3}^e(R < R_{ac}) \approx \hat{T}_e \Phi_R^{(2)}(r)/\Phi_R^{(2)}(r)$  and  $Q_{2,3}^e(R > R_{ac}) \approx \hat{T}_e \Phi_R^{(1)}(r)/\Phi_R^{(1)}(r)$ . Therefore, as can be seen from Fig. 2 (bottom left panel), the  $\mathbb{C}$ -TDPEs resemble diabatic potential-energy surfaces, coinciding with  $\epsilon_{BO}^{(2)}$  for  $R < R_{ac}$  and smoothly going through the avoided crossing region to follow  $\epsilon_{BO}^{(1)}$  for  $R > R_{ac}$ . The trajectory  $(r_1, R_1)$  tunnels from one Coulomb potential well  $W_\alpha$  to the other, staying most of the time in the support of  $\Phi_R^{(2)}(r)$ . The velocity  $\dot{r}_1$  is now large due to the fast re-configuration of the electronic degrees of freedom, and

hence  $V_1$  shows important advective contributions. Notice also that both  $V_1^{\Re}$  and  $V_1^{\Im}$  show steep peaks that originate in the full configuration space as the full probability density starts to split along the electronic coordinates (left panels b) and c) of Fig. 2). At the later time  $t = 19.32$ fs, the advective correlation and classical kinetic terms become once more negligible, and therefore  $V_\alpha \approx V_{\alpha,app}^{\Re} + V_{\alpha,app}^{\Im}$ . While  $(r_1, R_1)$  stays preferentially in the support of  $\Phi_R^{(2)}(r)$ , the trajectories  $(r_2, R_2)$  and  $(r_3, R_3)$  are mainly sampling the support of  $\Phi_R^{(1)}(r)$  (see the right panel of Fig. 1). The conditional wavefunctions  $\psi_1, \psi_2$  and  $\psi_3$  are now linear combinations of  $\Phi_R^{(2)}(r)$  and  $\Phi_R^{(1)}(r)$  [36]. This mixture leads to the formation of the step observed for  $V_1$  around  $R = 1.5a_0$ , and two wiggles accompanying the  $\mathbb{C}$ -TDPEs  $V_2$  and  $V_3$ . All these features indicate the nonadiabatic nature of the conditional wavefunctions and can be directly associated with the formation of nodes in the full probability density. Concretely, as shown in panels b) and c) of Fig. 2, the splitting of the full probability density can be understood as the result of the formation of dynamical nodes (originating from kinetic correlations) that move across the full configuration space as if they were knife edges. Finally, at time  $t = 31.5$  fs, the full molecular wavefunction has been split both along the electronic and nuclear directions. While the three conditional wavefunctions,  $\psi_1, \psi_2$  and  $\psi_3$ , still embody contributions from both  $\Phi_R^{(1)}(r)$  and  $\Phi_R^{(2)}(r)$ , these contributions are now very well separated along the nuclear coordinates with a minimum at around  $R_{sp} = 4a_0$  (see also Fig. 1, right panel). For nuclear coordinates less than  $R_{sp}$ , the support of the full probability density perfectly fits in the support of the first excited Born-Oppenheimer state  $\Phi_R^{(2)}(r)$ , while for  $R > R_{sp}$  it mainly falls in the ground state  $\Phi_R^{(1)}(r)$ . As a direct consequence, the quantum electronic potential acquires a discontinuity, i.e.  $Q_\alpha^e(R < R_{sp}) \approx \hat{T}_e \Phi_R^{(2)}(r)/\Phi_R^{(2)}(r)$  while  $Q_\alpha^e(R > R_{sp}) \approx \hat{T}_e \Phi_R^{(1)}(r)/\Phi_R^{(1)}(r)$ . The real parts of the  $\mathbb{C}$ -TDPEs are therefore piecewise connecting adiabatic surfaces, i.e.  $V_\alpha^{\Re} \approx V_{\alpha,app}^{\Re} \approx \epsilon_{BO}^{(1)}$  for  $R > R_{sp}$ , and  $V_\alpha^{\Re} \approx V_{\alpha,app}^{\Re} \approx \epsilon_{BO}^{(2)}$  for  $R < R_{sp}$  (see Ref. [35] for further discussion). In the transition between this two regions (at around  $R_{sp}$ ), the conditional wavefunctions  $\psi_1, \psi_2$  and  $\psi_3$  become linear combinations of (at least) the lowest two adiabatic states. As a result, the  $\mathbb{C}$ -TDPEs exhibit abrupt peaks, both real and imaginary, mainly originating from the potentials  $Q_\alpha^e$  and  $K_\alpha^{\Im}$ . In the full configuration space (left panels in Fig. 2), these features are translated into deep wells/barriers that keep the full probability density well separated into three pieces.

In view of the above discussion, the characteristic features of an ensemble of  $\mathbb{C}$ -TDPEs of the CD framework during a nonadiabatic transition are very similar to that of the gauge invariant part of the exact TDPE [34, 37, 38] within the EF framework: while in the

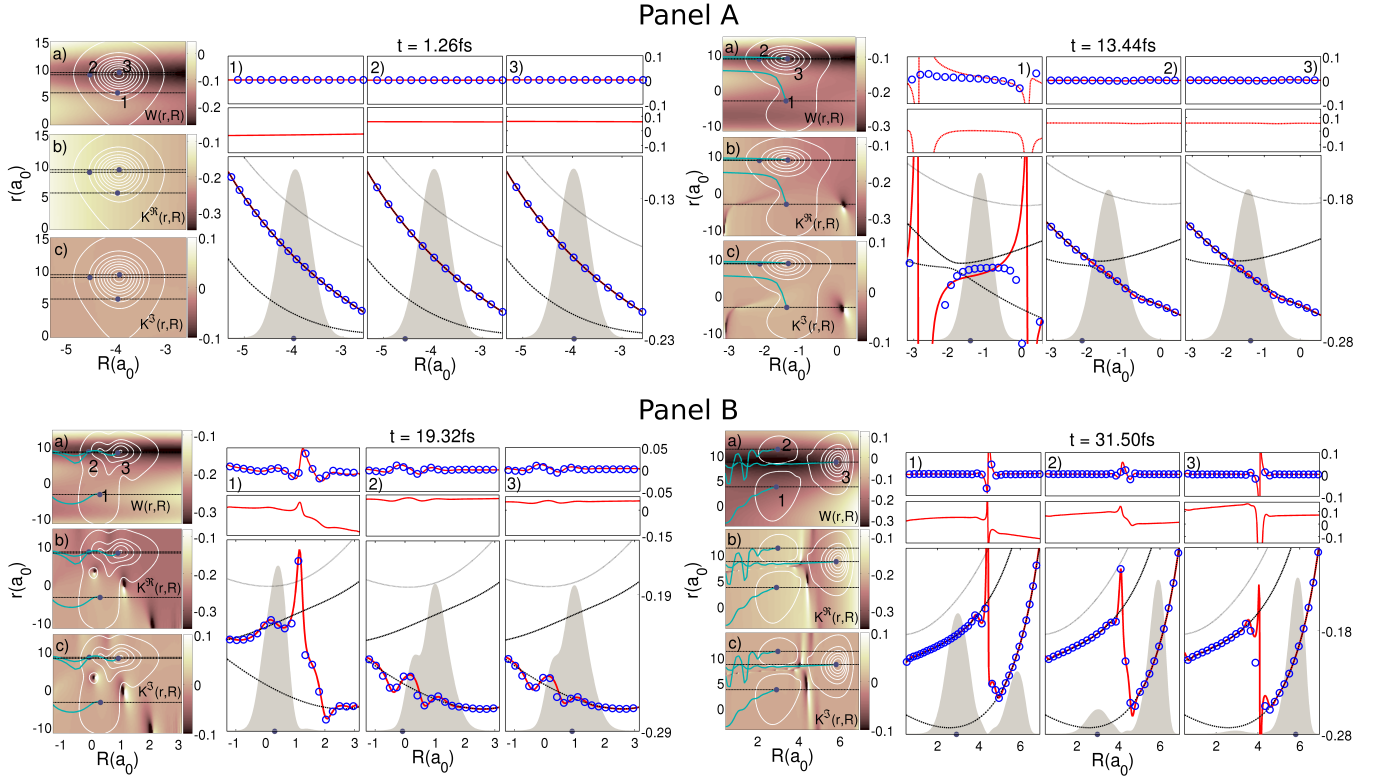


FIG. 2. PANEL A: Nuclear dynamics before the splitting of the probability density is mainly characterized by  $\mathbb{C}$ -TDPEs smoothly connecting  $\epsilon_{BO}^{(2)}$  and  $\epsilon_{BO}^{(1)}$ . PANEL B: Nuclear dynamics during the splitting of the probability density is accompanied by discontinuous steps in the  $\mathbb{C}$ -TDPEs piecewise connecting  $\epsilon_{BO}^{(2)}$  and  $\epsilon_{BO}^{(1)}$ . PANELS a,b,c: Contour lines of the full electron-nuclear probability density (in white) together with three conditional wavefunctions,  $\psi_1(R, t)$ ,  $\psi_2(R, t)$ , and  $\psi_3(R, t)$  (black lines), defined along with trajectories  $\{r_{\alpha=1,2,3}, R_{\alpha=1,2,3}\}$  (in cyan). In the background (in copper color scale), full (2D) dependence of a) the electron-nuclear potential energy  $W(r, R)$ , and b) and c) respectively the real and imaginary components of the kinetic correlation potential  $K(r, R, t)$ . PANELS 1,2,3 (bottom): Conditional probability densities  $|\psi_{\alpha=1,2,3}(R, t)|^2$  (filled in gray) along with the first three BOPEs (in black) and the real part of the  $\mathbb{C}$ -TDPEs  $V_{\alpha}^{\Re} = W_{\alpha} + K_{\alpha}^{\Re} + A_{\alpha}^{\Re}$  (in red). For comparison we also show the potential  $V_{\alpha,app}^{\Re} = Q_{\alpha}^e + W_{\alpha}$  (blue circles). PANELS 1,2,3 (middle): Electronic quantum potential  $Q_{\alpha}^e$ . PANELS 1,2,3 (top): Imaginary part of the  $\mathbb{C}$ -TDPEs  $V_{\alpha}^{\Im} = K_{\alpha}^{\Im} + A_{\alpha}^{\Im}$  (red line) along with the approximated potential  $V_{\alpha,app}^{\Im} = K_{\alpha}^{\Im}$  (blue circles).

vicinity of the avoided crossing both potentials follow a diabatic shape, far from the region of avoided crossings (when the nonadiabatic couplings are negligible) they are piecewise identical with two different adiabatic BOPEs with nearly discontinuous steps in between. By discussing the link between the potentials of the EF and CD approaches, in the remaining part of the Letter we elaborate on the origin of the discontinuities, which seem to be a universal feature of the time-dependent potentials driving the nuclear dynamics within formally exact approaches to correlated electron-nuclear dynamics.

The exact TDPE that governs the nuclear dynamics together with a vector potential within the EF framework, consists of two parts [34, 37, 38], the gauge invariant term,  $\epsilon_{gi}(\mathbf{R}, t)$ , and a gauge dependent term (see Ref. [39] for more details). By virtue of the EF theorem, the conditional nuclear wavefunction can be written as a direct product of conditional electronic and nuclear

wavefunctions, i.e.,  $\psi_{\alpha}(\mathbf{R}, t) = \Phi_{\mathbf{R}}(\mathbf{r}_{\alpha}, t)\chi(\mathbf{R}, t)$ . Hence,  $\epsilon_{gi}(\mathbf{R}, t)$  can be expressed in terms of  $\mathbb{C}$ -TDPEs and conditional nuclear wavefunctions,  $\psi_{\alpha}(\mathbf{R}, t)$ , as:

$$\epsilon_{gi}(\mathbf{R}, t) = \frac{\int \hat{\mathcal{D}}_{\mathbf{r}}[|\psi_{\alpha}|^2 V_{\alpha}] d\mathbf{r}}{\int \hat{\mathcal{D}}_{\mathbf{r}}[|\psi_{\alpha}|^2] d\mathbf{r}} + O(M_n^{-1}). \quad (6)$$

As the second term,  $O(M_n^{-1})$ , is mostly negligible due to its dependence on the inverse of the nuclear mass, the first term on the r.h.s of Eq. (6) establishes a direct connection between the gauge invariant part of the TDPE and the  $\mathbb{C}$ -TDPEs:  $\epsilon_{gi}(\mathbf{R}, t)$  is an ensemble average of  $\mathbb{C}$ -TDPEs,  $V_{\alpha}$ , which are integrated along the conditional probability densities  $|\psi_{\alpha}|^2$  and are weighted afterwards by the nuclear probability density,  $\int \hat{\mathcal{D}}_{\mathbf{r}}[|\psi_{\alpha}|^2] d\mathbf{r} = \int |\Psi|^2 d\mathbf{r}$ . As  $\int \hat{\mathcal{D}}_{\mathbf{r}}[|\psi_{\alpha}|^2 V_{\alpha}^{\Im}] d\mathbf{r}$  is zero (see Ref. [39]), Eq. (6) can be written as  $\epsilon_{gi}(\mathbf{R}, t) \approx \frac{\int \hat{\mathcal{D}}_{\mathbf{r}}[|\psi_{\alpha}|^2 V_{\alpha}^{\Re}] d\mathbf{r}}{\int \hat{\mathcal{D}}_{\mathbf{r}}[|\psi_{\alpha}|^2] d\mathbf{r}}$ . Furthermore, the electronic quantum potentials are the

main source of the discontinuities of  $V_{\alpha}^{\mathfrak{R}}$  as discussed before. Hence, the steps in  $\epsilon_{gi}(\mathbf{R}, t)$  can be viewed as an ensemble average of the discontinuities of the electronic quantum potential.

The branching of nuclear wavepackets during nonadiabatic transitions is traditionally described within the Born-Oppenheimer picture, in which the nuclear wavepacket can populate different BOPEs and in this way reproduce a coherent wavepacket branching. The same physics is described by single effective time-dependent potentials that drive the nuclear dynamics within the EF and CD frameworks through abrupt steps that connect the adiabatic pieces of the time-dependent potentials. In this work, we have presented characteristic features of the exact C-TDPESs for the specific situation where nonadiabatic transitions occur and the nuclear wavepacket branches. Within the CD framework, an ensemble of C-TDPESs govern the dynamics of the conditional nuclear wavefunctions and provides us with an alternative approach to study nonadiabatic processes. In this Letter, we have shown that C-TDPESs in the vicinity of an avoided crossing follow a diabatic shape, while far from the region of avoided crossings they are, piecewise, on top of one of the adiabatic BOPEs with a nearly discontinuous step that connects two different adiabatic BOPEs. These features of the exact C-TDPESs are equivalent to that of the gauge invariant part of the exact TDPEs within the EF framework. In this respect, we have demonstrated that the discontinuous step that connects two adiabatic pieces of the TDPEs within the EF framework can be reproduced by an ensemble average of the discontinuities of the C-TDPESs. Our study reveals that the shape and position of discontinuous steps are mainly dictated by the electronic quantum potential,  $Q_{\alpha}^e$ , and hence, they are universal. Moreover, this is a clear signature of the ultimate quantum nature of electron-nuclear correlations, i.e., within the CD and EF frameworks, the effective (nuclear) potentials have a direct dependence on the full wavefunction through the electronic quantum potential, which can induce discontinuities.

It is worth mentioning that other attempts to reduce the complexity of the time-dependent Schrödinger equation, such as in time-dependent density-functional theory, also lead to the emergence of striking discontinuities in the effective time-dependent potentials that govern the reduced variables of interest. This is the case, e.g., in the field of electron-electron correlated dynamics, where the nature of such discontinuities is currently under study [40–42].

**Acknowledgements:** G.A acknowledges financial support from the Beatriu de Pinós program through the Project: 2014 BP-B 00244. I.T acknowledges the Swiss National Science Foundation (SNF) through Grant No. 200021-146396. A.R acknowledges financial support from the European Research Council Ad-

vanced Grant DYNamo (ERC-2010- AdG-267374), Spanish Grant (FIS2013-46159-C3-1-P) and Grupos Consolidados UPV/EHU del Gobierno Vasco (IT578-13). We finally acknowledge COST Actions CM1204 (XLIC) and MP1306 (EUSpec).

---

\* albarda@ub.edu

† aliabedik@gmail.com

‡ ita@zurich.ibm.com

§ angel.rubio@mpsd.mpg.de

- [1] J. Clark, T. Nelson, S. Tretiak, G. Cirmi, and G. Lanzani, *Nature Physics* **8**, 225 (2012).
- [2] X. Zhou, P. Ranitovic, C. Hogle, J. Eland, H. Kapteyn, and M. Murnane, *Nature Physics* **8**, 232 (2012).
- [3] S. R. Leone, C. W. McCurdy, J. Burgdörfer, L. S. Cederbaum, Z. Chang, N. Dudovich, J. Feist, C. H. Greene, M. Ivanov, R. Kienberger, *et al.*, *Nature Photonics* **8**, 162 (2014).
- [4] F. Lépine, M. Y. Ivanov, and M. J. Vrakking, *Nature Photonics* **8**, 195 (2014).
- [5] R. Boge, C. Cirelli, A. Landsman, S. Heuser, A. Ludwig, J. Maurer, M. Weger, L. Gallmann, and U. Keller, *Physical review letters* **111**, 103003 (2013).
- [6] M. Corrales, J. González-Vázquez, G. Balerdi, I. Solá, R. de Nalda, and L. Bañares, *Nature chemistry* **6**, 785 (2014).
- [7] I. Tavernelli, *Accounts of chemical research* **48**, 792 (2015).
- [8] M. Persico and G. Granucci, *Theoretical Chemistry Accounts* **133**, 1 (2014).
- [9] B. Lasorne, G. A. Worth, and M. A. Robb, in *Molecular Quantum Dynamics* (Springer, 2014) pp. 181–211.
- [10] W. Domcke and D. R. Yarkony, *Annual review of physical chemistry* **63**, 325 (2012).
- [11] J. C. Tully, *The Journal of chemical physics* **137**, 22A301 (2012).
- [12] D. Truhlar, in *The Reaction Path in Chemistry: Current Approaches Understanding Chemical Reactivity*, Vol. 16, edited by D. Heidrich (Springer Netherlands, 1995) pp. 229–255.
- [13] B. F. E. Curchod, U. Rothlisberger, and I. Tavernelli, *ChemPhysChem* **14**, 1314 (2013).
- [14] J. C. Tully, *J. Chem. Phys.* **93**, 1061 (1990).
- [15] J. C. Tully, *Farad. Discuss.* **110**, 407 (1998).
- [16] R. Kapral and G. Ciccotti, *The Journal of chemical physics* **110**, 8919 (1999).
- [17] M. Persico and G. Granucci, *Theoretical Chemistry Accounts* **133**, 1 (2014).
- [18] S. Sawada and H. Metiu, *J. Chem. Phys.* **84**, 227 (1986).
- [19] T. J. Martinez, M. Ben-Nun, and R. D. Levine, *J. Phys. Chem.* **100**, 7884 (1996).
- [20] J. Zheng, X. Xu, R. Meana-Paneda, and D. G. Truhlar, *Chem. Sci.* **5**, 2091 (2014).
- [21] I. Burghardt, H.-D. Meyer, and L. S. Cederbaum, *J. Chem. Phys.* **111**, 2927 (1999).
- [22] M. Beck, A. Jckle, G. Worth, and H.-D. Meyer, *Phys. Rep.* **324**, 1 (2000).
- [23] H.-D. Meyer and G. A. Worth, *Theor. Chem. Acc.* **109**, 251 (2003).
- [24] A. Abedi, N. T. Maitra, and E. K. U. Gross, *Phys. Rev.*

- Lett. **105**, 123002 (2010).
- [25] G. Albareda, H. Appel, I. Franco, A. Abedi, and A. Rubio, Phys. Rev. Lett. **113**, 083003 (2014).
- [26] The electronic support of the full probability density  $|\Psi(\mathbf{r}, \mathbf{R}, t)|^2$  can be defined as:  $\text{supp}(|\Psi(\mathbf{r}, \mathbf{R}, t)|^2) = \{\mathbf{r} \in \mathbf{r} \mid |\Psi(\mathbf{r}, \mathbf{R}, t)|^2 > \lambda\}$ , where  $\lambda$  denotes a given lower bound of the probability density.
- [27] X. Oriols and J. Mompart, Applied Bohmian Mechanics: From Nanoscale Systems to Cosmology (Pan Stanford, 2012).
- [28] A. Benseny, G. Albareda, S. Sanz, J. Mompart, and X. Oriols, The European Physical Journal D **68**, 286 (2014), 10.1140/epjd/e2014-50222-4.
- [29] G. Albareda, J. M. Bofill, I. Tavernelli, F. Huarte-Larraaga, F. Illas, and A. Rubio, The Journal of Physical Chemistry Letters **6**, 1529 (2015), pMID: 26263307, <http://dx.doi.org/10.1021/acs.jpcclett.5b00422>.
- [30] G. Albareda, J. Suñé, and X. Oriols, Phys. Rev. B **79**, 075315 (2009).
- [31] G. Albareda, D. Marian, A. Benali, S. Yaro, N. Zangh, and X. Oriols, J. Comp. Electr. **12**, 405 (2013).
- [32] X. Oriols, Phys. Rev. Lett. **98**, 066803 (2007).
- [33] S. Shin and H. Metiu, J. Chem. Phys. **102**, 9285 (1995).
- [34] A. Abedi, F. Agostini, Y. Suzuki, and E. K. U. Gross, Phys. Rev. Lett. **110**, 263001 (2013).
- [35] (), see Appendix A in the SM for a detailed analysis of the C-TDPESs in terms of the Born-Huang expansion of the molecular wavefunction.
- [36] As shown in Ref. [35], the conditional wavefunctions can be always written as a linear combination of Born-Oppenheimer states, i.e.  $\psi_\alpha(r, t) = \sum_j C_j(R, t) \Phi_R^{(j)}(r_\alpha)$ .
- [37] A. Abedi, N. T. Maitra, and E. K. U. Gross, The Journal of Chemical Physics **137**, 22 (2012).
- [38] F. Agostini, A. Abedi, Y. Suzuki, S. K. Min, N. T. Maitra, and G. E. K. U., J. Chem. Phys. **142**, 084303 (2015).
- [39] (), see Appendix B in the SM for a detailed derivation of the connection between the C-TDPESs of the CD and the exact TDPEs of the EF.
- [40] P. Elliott, J. I. Fuks, A. Rubio, and N. T. Maitra, Physical review letters **109**, 266404 (2012).
- [41] K. Luo, P. Elliott, and N. T. Maitra, Physical Review A **88**, 042508 (2013).
- [42] K. Luo, J. I. Fuks, E. D. Sandoval, P. Elliott, and N. T. Maitra, The Journal of chemical physics **140**, 18A515 (2014).